# Stratigraphy, structure, and potassic alteration of Miocene volcanic rocks in the Sleeping Beauty area, central Mojave Desert, California

ALLEN F. GLAZNER *Department of Geology, CB 3315, Mitchell Hall, University of North Carolina, Chapel Hill, North Carolina 27599*

## ABSTRACT

**The Sleeping Beauty area of the southeastern Cady Mountains, central Mojave Desert, contains a sequence of volcanic rocks >3 km thick which was erupted approximately 20 m.y. ago. Plate reconstructions indicate that the change from subduction to transform-fault tectonics off the coast of California occurred about 20 m.y. ago as well, and so these rocks contain a record of volcanism, extensional faulting, and potassic metasomatism during this time of tectonic transition.**

**The volcanic sequence comprises basalt to rhyolite flows and tuffs which are overlain by the widespread Peach Springs Tuff and by terrestrial sediments. Bedding below the Peach Springs Tuff generally dips 10°–50° to the southwest and is cut by numerous steep northwest- to north-trending faults. Tilting predated deposition of the Peach Springs Tuff. Bedding-fault relationships indicate that deformation was not by "tilted-book" geometry in its simplest form. No significant low-angle faults are exposed, but such faults occur to the west and may underlie the area. A major open, southeast-trending anticline in the area may be a drag fold related to the post–late Miocene, right-lateral, north-trending Ludlow fault.**

**All units below the Peach Springs Tuff were locally affected by severe potassic metasomatism, which raised measured $K_2O$ contents to as high as 13.3 wt%. Metasomatized rocks occur in irregular zones that follow northwest-trending faults and are best developed around northwest-trending breccia zones which have jasper matrices. Ba and Mn prospects are invariably found in metasomatized rocks. Geologic and geochemical constraints indicate that metsomatism occurred at shallow depth (<1 or 2 km) and low temperature (<150 °C). Metasomatism occurred in at least two distinct pulses and apparently predated deposition of the Peach Springs Tuff. The K may have been derived from percolating closed-basin brines or through hydrogen metasomatism of rocks deeper in the complex.**

## INTRODUCTION

Tertiary volcanism and extensional faulting in the southwestern United States occurred as a northward-moving wave which swept through the central Mojave Desert about 20 m.y. ago (Armstrong and Higgins, 1973; Glazner and Bartley, 1984). This wave apparently tracked the northward progression of the Mendocino triple junction and thus occurred during the change from subduction to transform-fault tectonics off the coast of California. Volcanic rocks and associated structures in the Mojave Desert record details of this plate reorganization. In spite of the tectonic significance of the Mojave region, however, there are few published studies of the petrology and structure of the Tertiary volcanic rocks found there.

The Sleeping Beauty area of the southeastern Cady Mountains (Figs. 1, 2) is a 90-$km^2$ region of tilted volcanic rocks which lies in the center of the Mojave Desert. This sequence of rocks is of particular interest because (1) rocks in the area record three distinct but closely spaced periods of volcanism and accompanying mineralization and coarse-clastic sedimentation; (2) the sequence was tilted by extensional faulting, and the timing of faulting can be tightly constrained; and (3) the volcanic rocks were affected by intense potassic metasomatism. Potassic metasomatism is now known to be widespread in the southwestern United States (Chapin and Glazner, 1983), and in most areas, metasomatism is associated with crustal extension. Field and petrographic relations of metasomatism are better displayed in the Sleeping Beauty area than in most of the other areas cited by Chapin and Glazner (1983).

This paper provides a summary of the geology of the Sleeping Beauty area. The goals of the study were to determine (1) the petrologic char-

TABLE 1. K-Ar AGE DETERMINATIONS

| Sample | 8-7 | 12-3 | AG-3 | 11-1A |
|---|---|---|---|---|
| Unit | FSB | FAS | DCM | PST |
| Material | pl | wr | wr | san |
| $K_2O$, wt% | 1.135 | 1.585 | 3.475 | 6.425 |
| $^{40}Ar^*$, $10^{-10}$ mol/g | 0.3257 | 0.4562 | 1.0145 | 1.862 |
| $\%^{40}Ar^*$ | 64 | 64 | 69 | 56 |
| $^{40}Ar^*/^{40}K \times 10^5$ | 116 | 116 | 118 | 117 |
| Age, m.y. | 19.8 | 19.9 | 20.2 | 20.0 |
| $\pm 2\sigma$ | 1.4 | 0.7 | 1.3 | 1.0 |

*Note:* FSB = formation of Sleeping Beauty Ridge, FAS = formation of Argos Station, DCM = dacite of Cady Mountains, PST = Peach Springs Tuff; $^{40}Ar^*$ = radiogenic argon; pl = plagioclase separate, wr = whole rock, san = sanidine separate; $^{40}K$ constants: $\lambda_\epsilon = 0.584 \times 10^{-10}$/yr, $\lambda_\beta = 4.720 \times 10^{-10}$/yr, atomic abundance = $1.19 \times 10^{-4}$; analyses by R. F. Marvin, H. H. Mehnert, and V. M. Merritt at U.S. Geological Survey laboratories.

**Additional material for this article (an appendix) may be obtained free of charge by requesting Supplementary Data 8804 from the GSA Documents Secretary.**

Geological Society of America Bulletin, v. 100, p. 424–435, 10 figs., 4 tables, March 1988.

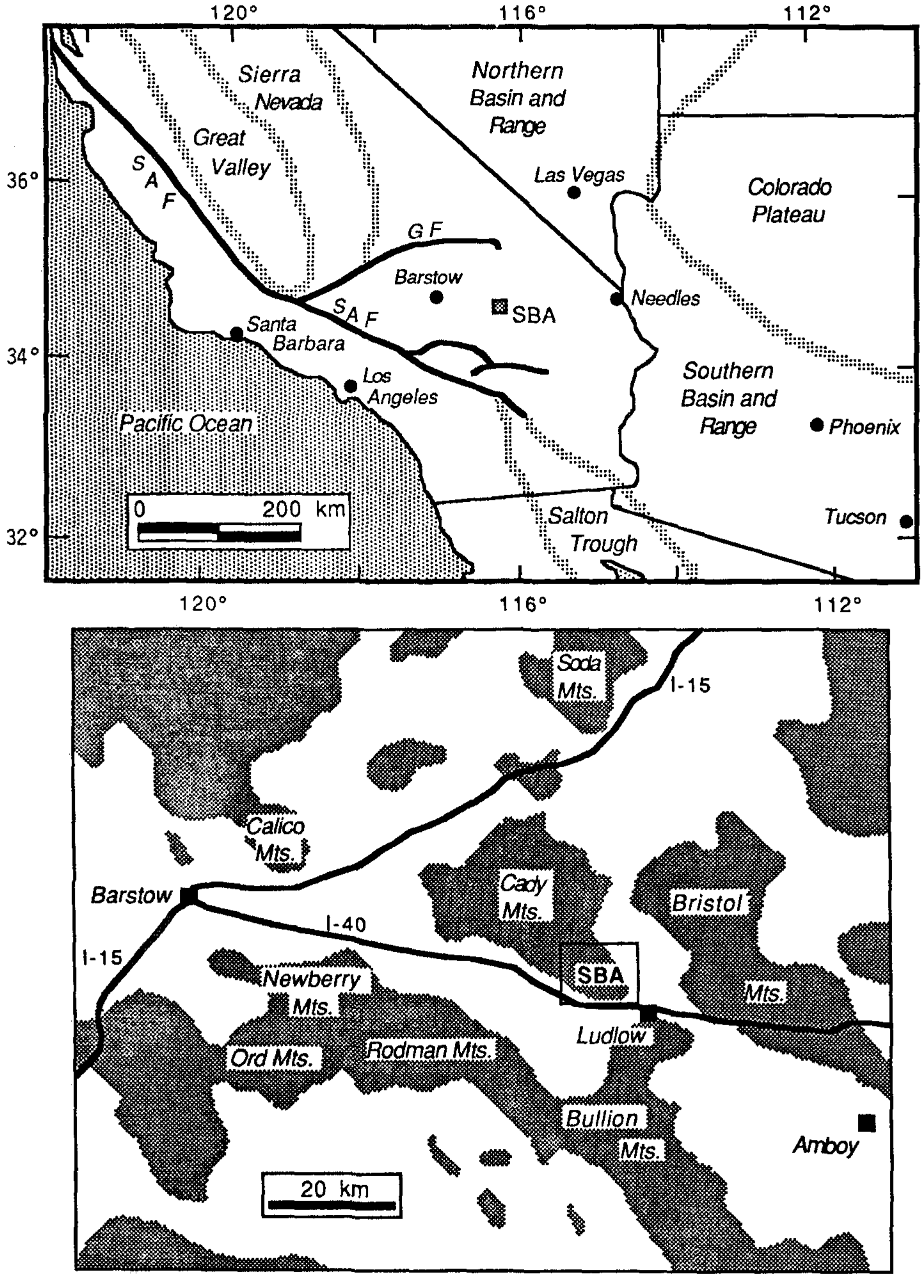


**Figure 1. Location of the Sleeping Beauty area (SBA) and associated tectonic elements of the southwestern United States. SAF = San Andreas fault; GF = Garlock fault.**

acter and age of Miocene volcanism in the area, (2) the nature and significance of potassic metasomatism in the area and its relationship to crustal extension and ore deposits, and (3) the structural style of Miocene deformation in the Sleeping Beauty area and its relationship to documented Tertiary extension in areas to the east (Davis and others, 1980), west (Dokka, 1986; Glazner and others, 1987), and north (Burchfiel and others, 1983). The petrology of fresh volcanic rocks in the Sleeping Beauty area will be discussed as part of a larger study of Miocene volcanism in the Mojave block (Glazner, 1988).

## VOLCANIC STRATIGRAPHY

The Sleeping Beauty area contains a sequence >3 km thick of lower Miocene lavas, pyroclastic rocks, and sediments which are tilted to the southwest at 10°–50°. Nowhere in the area is the Tertiary section seen in depositional contact with pre-Tertiary basement.

The five main units in the area, from oldest to youngest, are the formation of Sleeping Beauty ridge, the formation of Argos Station, the dacite of Cady Mountains, the Peach Springs Tuff, and the Hector Formation. The lower three are informal volcanic units.

The formation of Sleeping Beauty ridge is a heterogeneous assemblage of andesitic to dacitic flows and flow breccias, pyroclastic rocks, shallow intrusions, and volcaniclastic sediments. The distribution of facies within the unit defines a stratovolcano for which the center was near the southeast quarter of sec. 7, T. 8 N., R. 7 E. The formation of Argos Station comprises basalt to andesite flows and basalt scoria tuffs, silicic tuffs, and clastic sedimentary rocks. The dacite of Cady Mountains is a homogeneous unit composed of several thin flows of platy low-silica, high-K dacite which cover the southeastern part of the mapped area. The Peach Springs Tuff (defined by Young and Brennan, 1974) is a widespread rhyolite ignimbrite sheet in western Arizona which has recently been traced into the Mojave Desert (Glazner and others, 1986). The Hector Formation comprises fluvial, alluvial, and lacustrine sedimentary rocks that were originally defined by Woodburne and others (1974) for fossiliferous exposures in the western Cady Mountains.

K-Ar dates on single samples from each of the lower four units (Table 1) form a tight group ranging from 19.8 to 20.2 m.y. Most volcanic rocks in the east-west–trending belt running from the westernmost Mojave Desert east through Barstow to the Whipple and Mohave Mountains are 17–23 m.y. old (Glazner, 1988).

Detailed descriptions of the map units are available from the GSA Data Repository.[1] Major-element, trace-element, and Sr-isotopic data for fresh volcanic rocks from the Sleeping Beauty area are summarized in Table 2. The petrology of these rocks is discussed in Glazner (1988).

## STRUCTURAL GEOLOGY

The Sleeping Beauty area is dominated by northwest-trending, southwest-dipping bedding and by northwest- to north-striking steep faults. The style of deformation is similar to the "tilted-book" or "domino" geometry found in highly extended rocks of the southwestern United States (for example, Wernicke and Burchfiel, 1982). No major low-angle faults

[1]These analyses are available free of charge by requesting Supplementary Data 8804 from the GSA Documents Secretary.

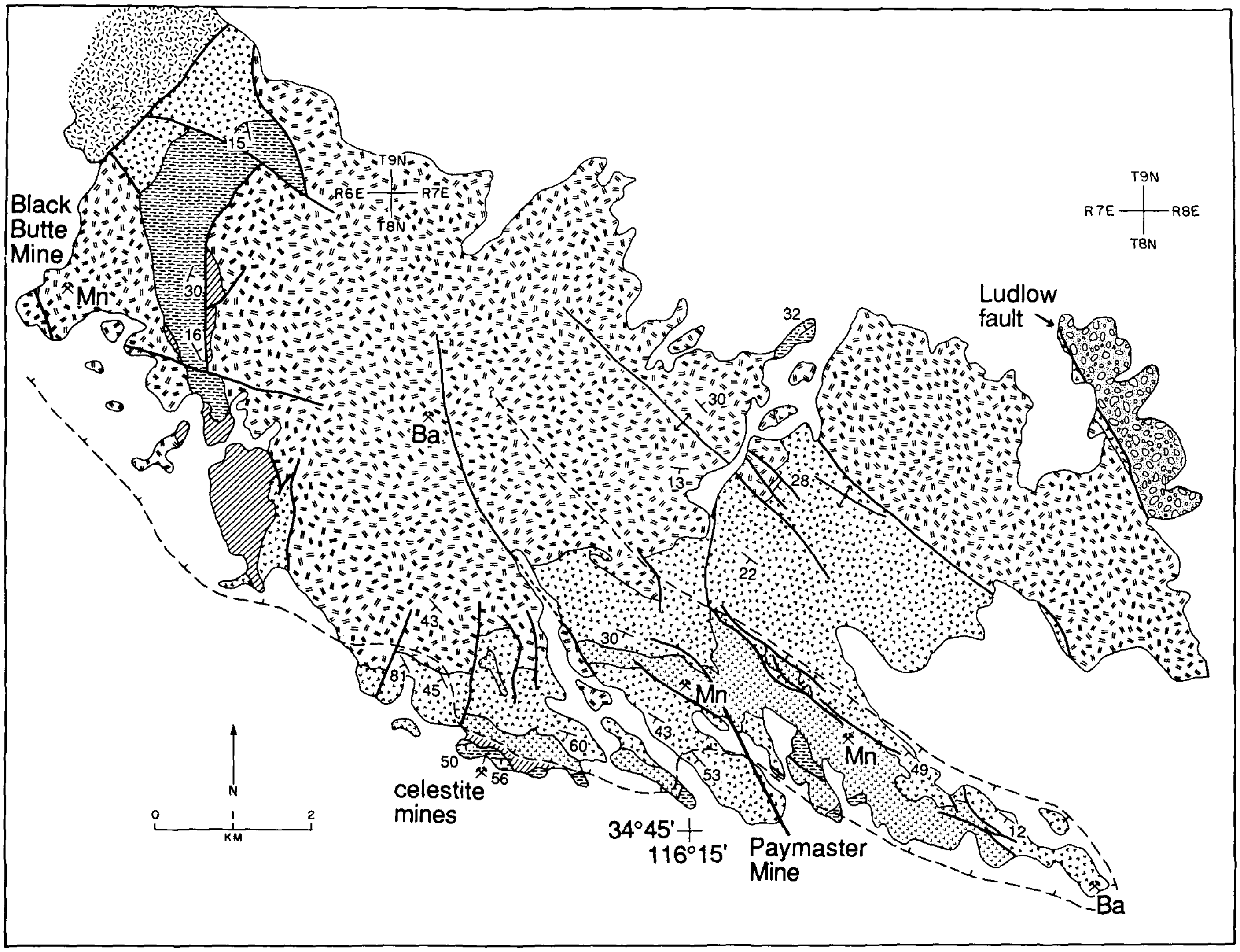


***QUATERNARY***

**ALLUVIUM**

***LATE TERTIARY OR QUATERNARY***

**FANGLOMERATE** Possibly equivalent to conglomerates of the Hector Formation

***EARLY MIOCENE***

**HECTOR FORMATION** Lacustrine limestone and siltstone and volcanic boulder conglomerate; siltstone facies locally contains nodules of celestite

**PEACH SPRINGS TUFF** Welded rhyolite tuff characterized by large (3-5 mm) sanidine phenocrysts with locally intense blue adularescence; minor sphene, biotite, hornblende, and plagioclase

**DACITE OF CADY MOUNTAINS** Aphanitic, flaggy dacite with sparse, small (<1 mm) phenocrysts of plagioclase and hypersthene; gray to red; locally a black vitrophyre which weathers chalky pink is developed

**FORMATION OF ARGOS STATION** Vesicular basalt and basaltic andesite; silicic air-fall and weakly welded ash-flow tuff; red to green sandstone; coarse conglomerate of both volcanic and granitoid detritus

**FORMATION OF SLEEPING BEAUTY RIDGE** Massive purple to red dikes, flows, and sills of andesite and dacite; green to purple tuff and tuff breccia; green sandstone and conglomerate beds; vent and flank facies of a stratovolcano

***MESOZOIC***

**GRANITOIDS OF THE CENTRAL CADY MOUNTAINS**

fault

contact

trace of axial plane of anticline

limits of area affected by strong K metasomatism

**Figure 2. Simplified geologic map of the Sleeping Beauty area.**

TABLE 2. REPRESENTATIVE MAJOR-ELEMENT, TRACE-ELEMENT, AND $^{87}Sr/^{86}Sr$ ANALYSES OF UNALTERED VOLCANIC ROCKS FROM THE SLEEPING BEAUTY AREA

| Unit | FAS | FAS | FAS | DCM | DCM | FSB | FSB | FSB | FSB | FSB |
|---|---|---|---|---|---|---|---|---|---|---|
| Sample | 11-90 | 12-3 | 13-22 | 13-21C | AG-2 | 10-5 | 25-13 | 82-22A | 82-25 | 9-4 |
| $SiO_2$ | 52.2 | 49.7 | 52.2 | 63.8 | 63.2 | 62.0 | 65.3 | 62.9 | 68.3 | 63.7 |
| $TiO_2$ | 2.11 | 2.63 | 2.21 | .88 | .76 | .94 | .42 | .84 | .40 | .71 |
| $Al_2O_3$ | 19.1 | 16.1 | 15.9 | 17.6 | 16.4 | 17.0 | 15.6 | 15.9 | 15.6 | 16.1 |
| $Fe_2O_3^t$ | 8.57 | 12.53 | 10.60 | 5.04 | 5.91 | 4.63 | 2.45 | 4.40 | 2.89 | 3.67 |
| MgO | 3.24 | 4.51 | 3.77 | .82 | 1.49 | 1.40 | 1.15 | 2.17 | 1.12 | 1.39 |
| CaO | 7.96 | 8.23 | 7.43 | 3.71 | 3.69 | 4.32 | 2.94 | 4.53 | 3.45 | 4.22 |
| $Na_2O$ | 4.05 | 3.67 | 3.77 | 4.67 | 5.01 | 4.51 | 4.04 | 4.05 | 4.09 | 4.00 |
| $K_2O$ | 1.75 | 1.53 | 2.06 | 3.69 | 3.20 | 1.44 | 3.53 | 3.18 | 4.09 | 1.95 |
| $P_2O_5$ | .22 | .55 | .49 | . . | .33 | .21 | .08 | .19 | .14 | .16 |
| LOI | .3 | -1.1 | .7 | . . | .3 | 2.0 | 1.7 | .8 | .9 | 1.3 |
| Total | 99.5 | 98.4 | 99.1 | 100.2 | 100.3 | 98.4 | 97.2 | 99.0 | 101.0 | 97.2 |
| Rb | 33 | 31 | 56 | 130 | 115 | 141 | 116 | 108 | 128 | 192 |
| Sr | 920 | 557 | 526 | 492 | 450 | 630 | 558 | 618 | 710 | 686 |
| Y | 28 | 30 | 30 | 33 | 35 | 20 | 14 | 21 | 20 | 18 |
| Zr | 158 | 202 | 217 | 337 | 339 | 209 | 151 | 192 | 178 | 185 |
| Zn | 71 | 114 | 94 | 74 | 59 | 45 | . . | . . | . . | 54 |
| Ba | 748 | 500 | 583 | 1190 | 981 | 944 | . . | . . | . . | 833 |
| $^{87}Sr/^{86}Sr$ | . . | .70550 | .70575 | .70893 | .70885 | . . | .70722 | .70756 | .70723 | .70783 |

*Note:* FSB = formation of Sleeping Beauty Ridge; FAS = formation of Argos Station; DCM = dacite of Cady Mountains. LOI = loss (or gain) on ignition; · · = not determined. Major- and trace-element analyses by X-ray fluroescence and, on some samples, by atomic absorption for Na and Mg. Oxides in weight percent; trace elements in parts per million. Isotopic ratios are measured values (not corrected for age).

were found in the area, and none of the faults examined is demonstrably listric. It is probable, however, that a major low-angle fault or fault set which accommodates the tilting underlies the area. Low-angle faults which project under the Sleeping Beauty area are found in ranges several tens of kilometres to the west, in the Newberry Mountains and Waterman Hills (Dokka, 1986; Glazner and others, 1987).

Structural data for the Sleeping Beauty area are summarized in Figure 3. Mean bedding attitude is N74°W, 17° southwest, and poles to bedding define a great circle for which the axis plunges 7° to S50°E. Northeast dips reflect minor folding about southeast-trending axes.

## Faults

Faults are generally steep (Fig. 3). Their poles define a crude great circle, the axis of which is nearly horizontal and strikes S23°E. Thus, measured faults strike significantly more northerly than does bedding. In idealized "tilted-book" geometry, faults and bedding strike parallel to one another, and thus, the great circles corresponding to poles to faults and to poles to bedding should coincide. The discrepancy in the Sleeping Beauty area (Fig. 3) indicates that deformation was more complicated than a single episode of extension accompanied by rotation of faults and bedding about the same horizontal axis. Wells and Hillhouse (1986) reported that the paleomagnetic declinations recorded in Peach Springs Tuff in tilted ranges in the Colorado River trough, when corrected for dip by simple rotation around the strike line, are anomalous when compared to the declinations recorded in untilted outcrops. These data indicate that tilting of beds accompanied by net rotation about a vertical axis may be common in the Mojave region.

The discrepancy in strike between faults and bedding results in left-lateral separation of contacts of as much as 2 km and in repetition of the stratigraphic section in adjoining structural blocks. Slip directions on most of the faults are not well constrained. Their strikes are consistent with either dip slip related to early Miocene northeast-southwest extension or with right-

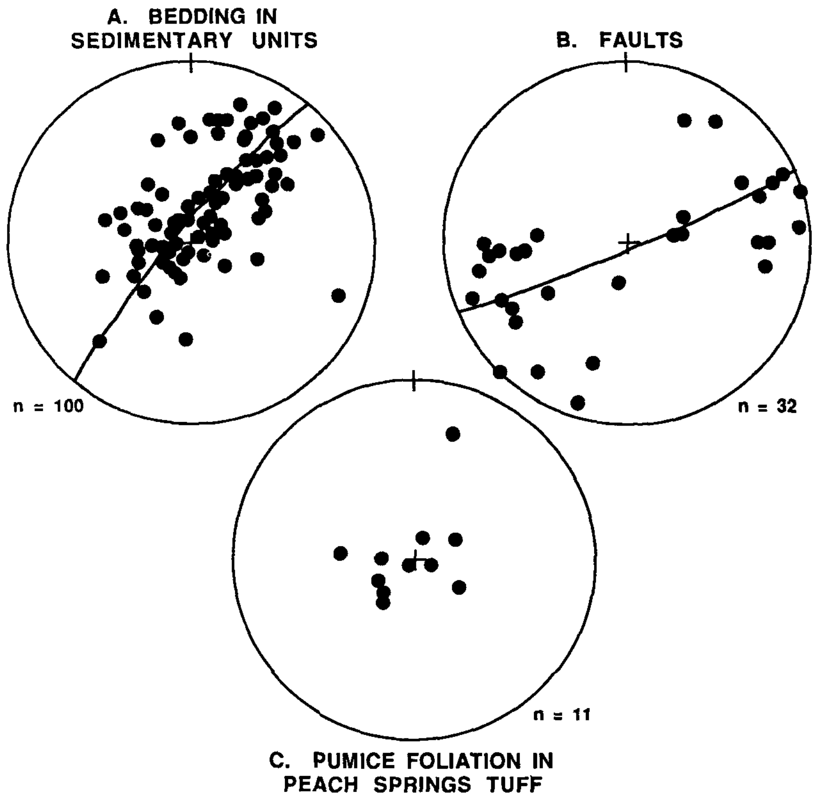


**Figure 3. Equal-area stereoplots of structural data from the Sleeping Beauty area. (A) Poles to sedimentary bedding in units below the Peach Springs Tuff; (B) poles to faults; (C) poles to pumice foliation in the Peach Springs Tuff. Scatter of poles to pumice foliation about the vertical in C indicates that tilting predated deposition of the Peach Springs Tuff. Best-fit great circles calculated by eigenvector method.**

lateral movement as part of the younger San Andreas fault system. Northwest-trending right-lateral faults are common in the Mojave Desert, and the Ludlow fault, which is assumed to be right lateral (Garfunkel, 1974), bounds the area on the east (Fig. 2). Measured slickensides are about evenly divided between those with horizontal rakes and those with rakes parallel to the dip direction. Two examined faults show horizontal slickensides cutting vertical slickensides. It is possible that many of the faults formed as dip-slip faults during early Miocene extension and then were reactivated as strike-slip components of the San Andreas system when the Gulf of California opened in the late Miocene.

The linear, west-northwest–trending southern boundary of the area (Figs. 1, 2) may mark the trace of a major fault. Bedding in the southwestern part of the area, near the celestite mines, dips as much as 70° to the south, in contrast to the gentler southwesterly dips prevalent elsewhere. In the alluvial basin south of the area and north of U.S. Interstate 40, the Peach Springs Tuff is intersected in drill holes at depths much less than those predicted by extrapolating the steeply dipping beds south under the alluvium (P. Wilkinson, 1983, oral commun.). Thus, the steep dips encountered near the celestite mines may be a result of drag along a basin-bounding fault.

A major northeast-trending fault juxtaposes Tertiary rocks of the Sleeping Beauty area with granitoids of the central Cady Mountains to the northwest. This fault, which is the only major northeast-trending fault in the area, truncates northwest-trending faults and is marked by a prominent fault-line scarp. Granitoids northwest of the fault rise >300 m above topographically subdued Hector Formation conglomerates to the southeast. Fault movement, or at least that portion of movement which juxtaposed the granitoids with the sedimentary rocks, probably postdated conglomerates of the Hector Formation because the conglomerates contain <1% granitoid clasts. Dokka (1986, Fig. 9) portrayed this fault as right lateral but did not document any slip indicators. A thorough study of exposures of the fault failed to support this claim. The kinematic significance of the fault is unknown. Because movement on it postdated deposition of the Peach Springs Tuff, and extension apparently ceased before deposition of the Peach Springs Tuff, it cannot be a tear fault related to extension.

### Folds

A major anticline and a small anticline-syncline pair, all of which have upright, southeast-trending axial planes, have folded Tertiary rocks in the Sleeping Beauty area. The large anticline plunges gently to the southeast and occupies the northeastern part of the area. The anticline-syncline pair has warped beds near the Paymaster Mine (sec. 21 and 27, T. 8 N., R. 7 E.).

The structural significance of the folding is unknown. The large anticline could be a drag fold related to the young Ludlow fault because it trends approximately 25°–30° to the fault and is in proper orientation for a drag fold related to a right-lateral fault (Moody and Hill, 1956). Alternatively, the fold may have formed in the compressional quadrant of the termination of the Ludlow fault because mapping by Dibblee (1967) shows that the Ludlow fault loses surface expression in the valley northeast of the Sleeping Beauty area. Tension gashes in the surface of Broadwell Lake (Dibblee, 1967), which lies immediately northeast of the area (Fig. 1), would then represent deformation in the complementary extensional quadrant.

### Timing of Deformation

Faulting and tilting were apparently largely complete by the time that the Peach Springs Tuff blanketed the area, because the tuff is tilted less than are older parts of the section. Pumice foliation, which is usually a reliable indicator of original horizontality in ash-flow tuffs, generally dips less than 25° and scatters about horizontal instead of dipping predominantly to the southwest as do underlying units (Fig. 3C). Peach Springs Tuff dips steeply only near the celestite mines in the southwestern part of the area, and as noted above, this is probably related to local fault drag. Some folding apparently predated deposition of the Hector Formation because south of the Paymaster Mine, Hector Formation sedimentary rocks lap discordantly on the dacite of Cady Mountains along the syncline axis. Because the Peach Springs Tuff is 18–19 m.y. old (Glazner and others, 1986) and older units are dated at 19.8–20.2 m.y. (Table 1), most deformation probably occurred 18–20 m.y. ago.

## MINERAL DEPOSITS

During the first half of the century, manganese oxides, celestite, and barite were taken from the Sleeping Beauty area. All mines are now idle. Mn oxides and barite occur as hydrothermal vein minerals, whereas celestite is found as nodules and seams in lacustrine sediments of the Hector Formation. Mn and Ba mineralization is restricted to a narrow, northwest-trending zone that extends from the Hansen barite prospect at the extreme southeastern tip of the area to the Black Butte Mn mine at the northwestern part of the area. The zone continues to the northwest, out of the Sleeping Beauty area, through the Logan Mn mine in the central Cady Mountains. Durrell (1953) described the geology of the lacustrine celestite deposits in detail.

A striking aspect of mineralization in the area, including the Logan Mn mine to the northwest, is that every Ba or Mn mine or prospect is found in volcanic rocks which have undergone strong potassic metasomatism. This implies that either the ores were carried in the same fluid as the K, or that the ores and K were carried in different fluids but used the same fracture system. In view of the one-to-one correspondence between ore deposition and metasomatism, and the geochemical similarities of Ba and K, the former seems more likely.

Barite occurs as veins as much as 1 m wide along shear zones in the formation of Sleeping Beauty ridge and the formation of Argos Station. These zones, which are part of the main fault system, generally strike northwest and dip steeply. Barite is commonly intergrown with jasper.

Veins of Mn oxides are most prevalent along shear zones in the dacite of Cady Mountains, although they are found in underlying units as well. Mn oxides and barite are rarely found in the same vein. The Mn deposits are surficial and apparently do not extend downward more than about 10 m (Trask, 1950, p. 195–200). The ore is locally accompanied by banded, white calcite.

It is possible that the Sr in sediments of the Hector Formation was derived from the volcanic pile during metasomatism because Sr was leached from the volcanic rocks during metasomatism (see below).

## POTASSIC METASOMATISM

Large parts of the Sleeping Beauty area, and all units below the Peach Springs Tuff, were affected by extreme potassic metasomatism (Fig. 2). Although these rocks were once thought to be highly anomalous and rare, they are now known to be widespread in the southwestern United States (Chapin and Glazner, 1983). Potassic rocks are significant because they may provide clues to the stress conditions under which low-angle normal faulting occurs (Bartley and Glazner, 1985). Potassic metasomatism is usually found in steeply tilted rocks, commonly in the hanging walls of low-angle normal faults.

Potassic Tertiary volcanic rocks in the Sleeping Beauty area and in the Picacho Peak area and Vulture Mountains of Arizona were originally thought to be primary high-K igneous rocks (Shafiqullah and others, 1976; Glazner and Stork, 1976; Rehrig and others, 1980), but further work has shown that these occurrences are metasomatized (Brooks, 1986; A. F. Glazner, unpub. data). Samples from the Picacho and Vulture localities are petrographically identical to those from the Sleeping Beauty area. Within the Mojave Desert, potassic rocks similar to those described below occur in the central Cady Mountains, at Sunshine Peak south of Pisgah Crater, and in the Waterman Hills north of Barstow. In the Waterman Hills, metasomatism occurs in steeply tilted to overturned rhyolites which lie immediately above the Waterman Hills detachment fault (Bartley and Glazner, 1987).

The alteration style seen in K-metasomatized rocks from the southwestern United States bears a striking resemblance to the alteration aureoles around shallow carbonatite complexes in eastern Africa (for example, Bailey, 1960; Garson, 1962; Brown, 1964). This observation, coupled with the strong enrichment of light rare earths in vein calcite from the Sleeping Beauty area, led to a suggestion that metasomatism in the Sleeping Beauty area was caused by a carbonatite (Glazner, 1979). Detailed mapping of the area has not revealed any further support for the carbonatite model, however.

## Field Characteristics

Metasomatized rocks in the Sleeping Beauty area are commonly reddened and brecciated, although metasomatized lithic tuffs of the formation of Argos Station are greenish. Metasomatism is best displayed in the field in the dacite of Cady Mountains, which forms gray to pale green slopes where unaltered and pink, purple, or red crags where altered. At several localities in the dacite, a striking color change from pale green to pink shows a one-to-one correspondence with degree of K enrichment. Lavas of the formation of Sleeping Beauty ridge and mafic flows of the formation of Argos Station are less obviously metasomatized because their dark colors are relatively unchanged by alteration.

Metasomatism is spatially associated with northwest-trending breccia zones and veins (Fig. 4), and the elongation of metasomatized zones is northwesterly, parallel to regional strike (Fig. 2). Rocks around the Logan Mn mine, a few kilometres northwest of the Sleeping Beauty area in the central Cady Mountains (Fig. 1), are also metasomatized. In highly brecciated areas within the dacite of Cady Mountains (for example, Fig. 4C), breccia clasts have pink rims containing about 12 wt% $K_2O$ which grade into pale green cores containing less than 4 wt% $K_2O$. The breccia zones and veins are invariably filled with dense to moderately porous brick-red jasper (Figs. 4A, 4C). Metasomatized zones range from millimetre-wide vein margins (Fig. 4B) to metre-wide zones adjacent to thick jasper-filled veins (Figs. 4A, 4C; referred to hereafter as "jasper-filled breccia zones") to entire hillsides of shattered, metasomatized rock in which the jasper breccia matrix is minor. Locally, the jasper matrix is present only as a fine hematite-like coating on breccia fragments. Similar jasper rocks are found in carbonatite complexes from Zambia (Bailey, 1960) and Tanzania (Brown, 1964).

The jasper-filled breccia zones are generally found only in the dacite of Cady Mountains, although in the southeastern part of the area, a few jasper-filled breccia zones cut the contact with the underlying formation of Argos Station. The breccia zones are best developed in the eastern wall of the canyon in the southeast quarter of sec. 21, T. 8 N., R. 7 E. Clasts in the breccia zones (Figs. 4A, 4C) generally match the dacite wall rocks but only rarely can the pieces be put back together. This indicates transport, mixing, and comminution of clasts in the breccia zones.

## Petrographic and Mineralogic Characteristics

Metasomatism is evident in thin section in the replacement of plagioclase by a nearly pure K-feldspar of intermediate to disordered structural state (hereafter termed "adularia") and in the oxidation and breakdown of mafic minerals (Fig. 5). Adularia is distinguishable from plagioclase by its small 2V (5°–20°), lower birefringence, negative optic sign, and lack of albite twinning. Carlsbad twinning and patchy extinction are common.

The composition of the adularia, measured using the electron microprobe, is $Or_{95}$–$Or_{100}$. Unit-cell parameters determined from whole-rock powder X-ray diffraction patterns are given in Table 3. The mean volume predicts a composition of $Or_{95}$ (Kroll and Ribbe, 1983). The cell parameters are slightly anomalous because a, b, and c do not conform to the correlation equation given by Kroll and Ribbe (1983, p. 82). On the basis of the determinative curves presented by Kroll and Ribbe, it appears that b is approximately 0.002 nm shorter than the value predicted from a, c, and the cell volume. Shortening of the b dimension has been attributed to substitution of boron for Al in some authigenic feldspars (Sheppard and Gude, 1965, 1973; Martin, 1971). The cell parameters determined in this study are virtually identical to those of synthetic B-bearing K-feldspars synthesized by Martin (1971). If the adularia is B bearing, then the composition estimated from the cell volume is an underestimate of the true Or content of the feldspar.

The b and c dimensions of the adularia indicate that it is moderately disordered (Kroll and Ribbe, 1983). This presents an apparent contradiction because it is likely that the adularia grew at low temperatures, and low-temperature feldspars are generally highly ordered. Several authors (for example, Sheppard and Gude, 1965; Koski and others, 1978; Kastner and Siever, 1979), however, have noted that metasomatic K-feldspar grown at low temperatures (<200 °C) may have disordered structure and optics. Kastner and Siever (1979) suggested that the lack of ordering in authigenic K-feldspars may result from kinetic effects because a certain amount of thermal energy is necessary to rearrange the Al and Si atoms into an ordered state.

Replacement of groundmass plagioclase is difficult to detect in thin section, but phenocrysts show the effects well (Fig. 5). The phenocryst replacement process takes one of two forms. Most commonly, a grainy texture develops in the outer zones of the phenocryst and forms a grainy area which surrounds a relic core of plagioclase (Fig. 5A). Backscatter scanning electron photomicrographs (Fig. 6) show that the grainy texture results from patchy replacement of original plagioclase by pure adularia, with the ratio of adularia to plagioclase increasing toward the grain margin. Less commonly, replacement begins at the grain margin and along cracks (Fig. 5B) and works inward without development of a grainy zone. Plagioclase phenocrysts that have been replaced are susceptible to plucking during thin-section preparation and in many cases show a boxwork texture (Fig. 5C).

The alteration of mafic minerals was not investigated in detail. In metasomatized rocks, mafic minerals are oxidized to clots of hematite and unidentified opaque alteration products which are pseudomorphs after hornblende and iddingsite. In some metasomatized basalts and andesites, celadonite is present as a vein filler and associated with opaque clots. An unexplained feature of the mineralogy of these rocks is the presence of minute flakes of phlogopite in the groundmass of both fresh and metasomatized samples of the dacite of Cady Mountains. The composition of the phlogopite in fresh and altered samples is identical [atomic ratios Mg/(Mg+Fe) = 0.71, K/Na = 6.4]. Either the phlogopite was unaffected by the metasomatic event (compare with Chapin and Lindley, 1986, who found that phenocrystic biotite is in many cases unaffected during metasomatism), or it was introduced after metasomatism occurred.

## Chemical Changes Accompanying Metasomatism

Several complete chemical analyses of the dacite of Cady Mountains (Table 2 and several untabulated analyses) indicate that it is homogeneous in its major- and trace-element composition. The chemical homogeneity and distinctive texture of the dacite make it an excellent control rock for studying alteration processes. The following section is based mainly on observations of this unit.

Metasomatism involved mobility of K and Rb, which were added, and of Na, Ca, Mg, and Sr, which were removed (Fig. 7). Zn is highly enriched in some samples (notably in the dacite of Cady Mountains) but not in all. Other measured major and trace elements did not vary

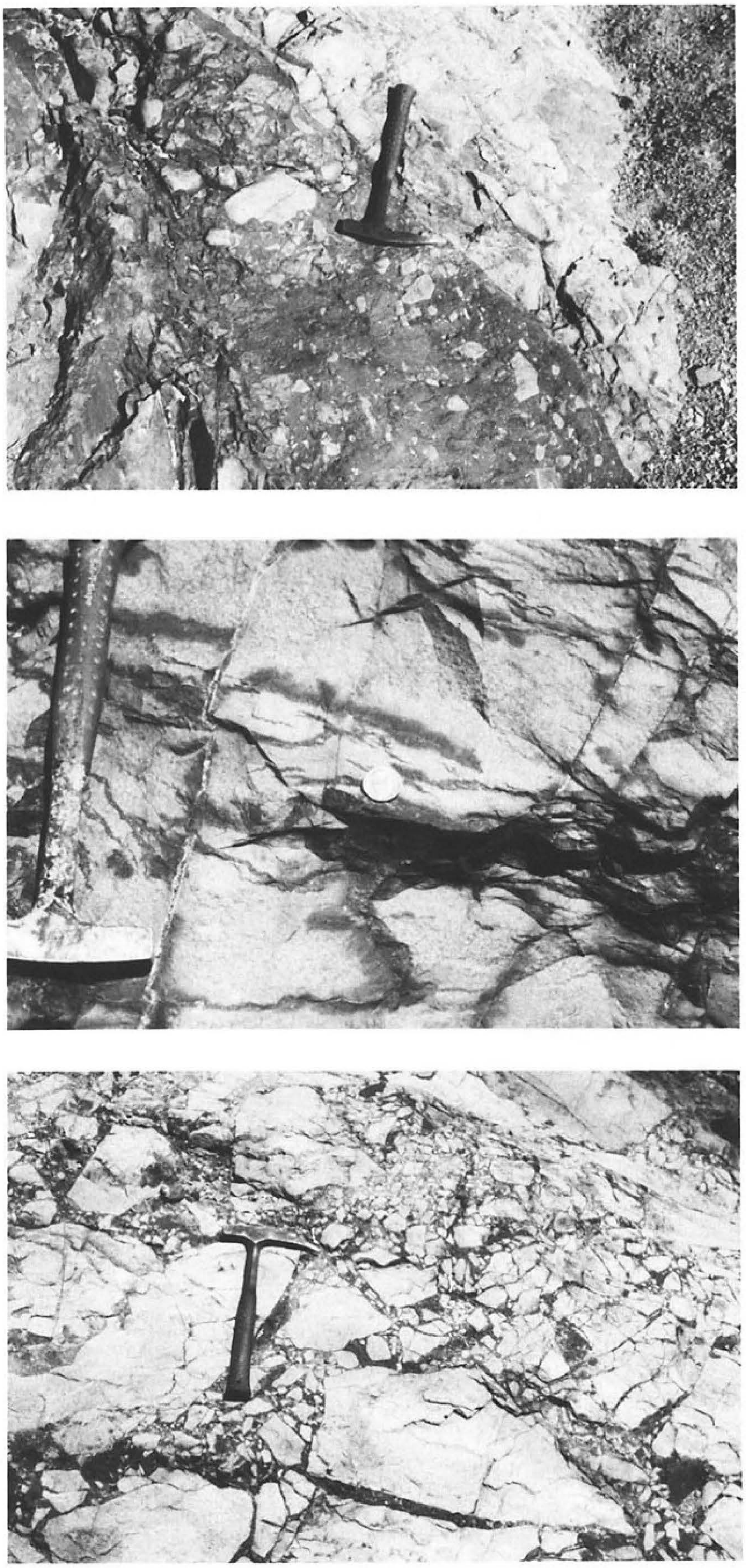

A

B

C

**Figure 4. Outcrop photographs of metasomatized rocks from the dacite of Cady Mountains. (A) Jasper-filled breccia zone intruding dacite. Hammer lies across the contact, with its head on jasper and handle on dacite. Clasts in this zone are all dacite and are uniformly pale purple owing to metasomatism. Dacite a few metres from the zone has 3.5 wt% $K_2O$; clasts contain 12 wt% $K_2O$. Results of analyses from this locality are in Table 4. (B) Incipient metasomatism in aphyric dacite near the Lavic Mountain manganese mine. Unmetasomatized green dacite is altered to dark red along thin cracks. Dark red areas are K metasomatized and oxidized. The volume increase accompanying metasomatism may promote brecciation (see text). (C) Highly brecciated dacite near the Paymaster manganese mine. Dark breccia matrix is quartz, ferric oxides, and manganese oxides; clasts are all shattered blocks of aphyric dacite. Clasts grade from light greenish-gray cores to light pink rims, reflecting an outward increase in metasomatism.**

substantially during metasomatism (Table 4). K and Rb were accommodated by adularia. Na, Ca, Mg, and Sr were removed by replacement of plagioclase and by breakdown of mafic minerals. The host for the added Zn is unknown. It may have accompanied Mn in Mn oxides.

Composition-volume relationships (Gresens, 1967; Appleyard and Woolley, 1979) can be used to infer volume changes during metasomatism. Gresens showed that the gain or loss of a chemical component during metasomatism can be expressed by the equation $(\Delta W_i)/W^0 = (V^d/V^p)(\rho^d/\rho^p)W_i^d - W_i^p$, where $\Delta W_i$ is the mass of component i removed or added, $W^0$ is the initial mass of the parent rock volume (commonly chosen to be 100 g, so that $\Delta W_i$ is in weight percent relative to the parent rock), $V^d$ and $V^p$ are the volumes of the daughter and parent rocks, $\rho^d$ and $\rho^p$ are their densities, and $W_i^d$ and $W_i^p$ are the mass fractions of component i in the daughter and parent rocks. Given chemical analyses and densities of daughter and parent rocks, one equation can be written for each chemical component. Immobility of an element requires that $\Delta W_i = 0$.

Composition-volume calculations for conversion of fresh dacite of Cady Mountains (sample 13-21C, Table 4) to its altered equivalent (sample 13-21B, Table 4) indicate that metasomatism was accompanied by a volume increase of about 14 vol%. This is shown in Figure 8, which is a summary of the volume factors ($V^d/V^p$) needed for immobility of each element. Several elements, including those which are commonly assumed to be relatively immobile in metaso-

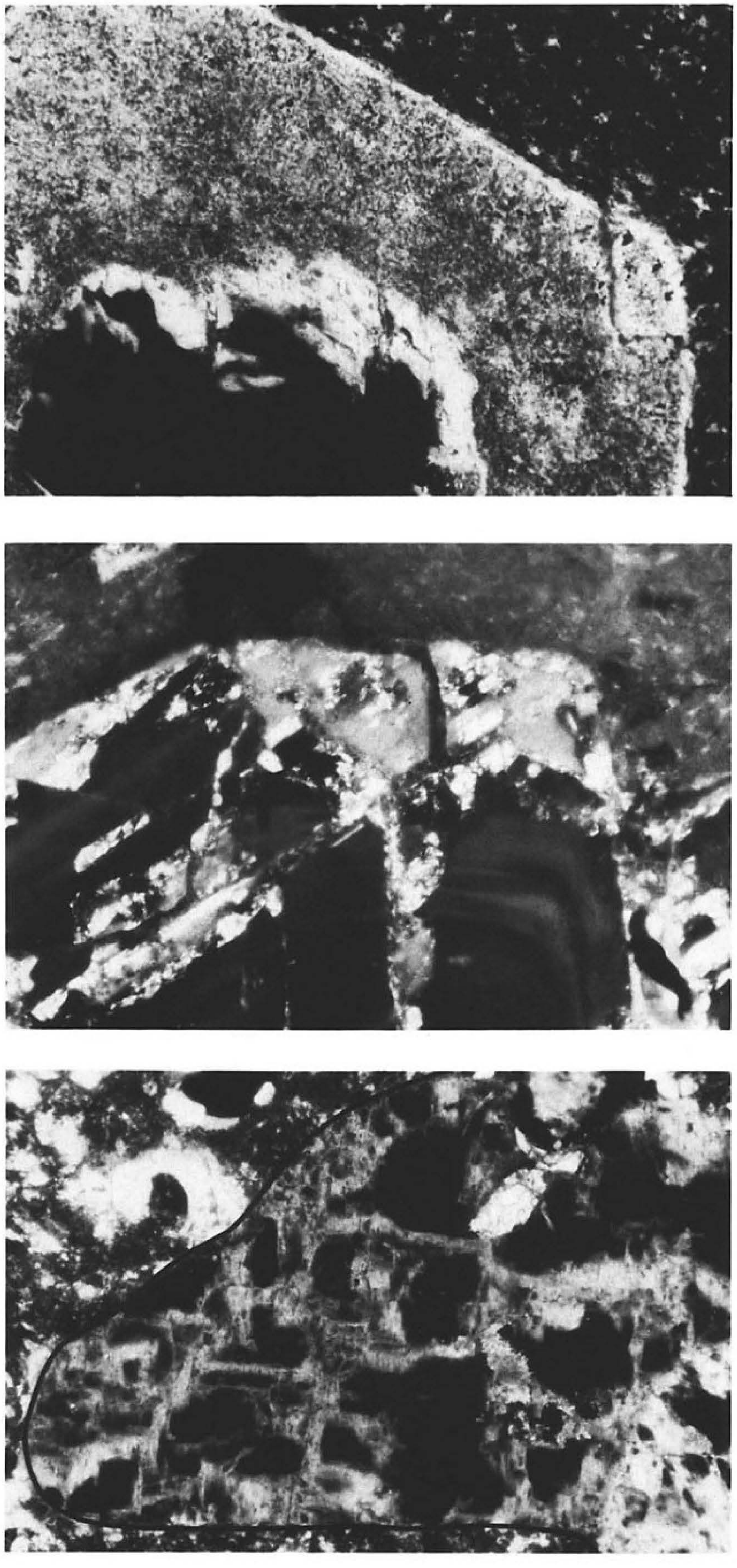

A

B

C

**Figure 5. Photomicrographs of metasomatized rocks from the Sleeping Beauty area and from the Vulture Mountains, Arizona. (A) Adularia replacing plagioclase in the dacite of Cady Mountains. This grain shows a plucked center (lower left), a plagioclase core (white), a grainy zone of mixed plagioclase and adularia, and a thin white rim of adularia. Width of field, 1.4 mm; crossed polarizers. (B) Thin, clear adularia rim on zoned plagioclase phenocryst in the formation of Sleeping Beauty ridge. Replacement occurs both at the rim and along cracks. Width of field, 0.7 mm; crossed polarizers. (C) Adularia (after plagioclase) from an andesite dike from the Vulture Mountains. Adularia lies within the black curve. Boxwork texture is caused by plucking and is characteristic of plagioclase that has been completely replaced. Width of field, 1.4 mm; crossed polarizers.**

matic processes (for example, Al, Ti, Zr, rare earths), cluster at volume factors slightly greater than unity. The geometric mean of volume factors needed for immobility of all measured elements except K, Rb, Zn, Sr, Na, Ca, and Mg is 1.14. Thus, Al, Ti, Zr, rare earths, and several other elements could have been immobile during metasomatism if the volume of the daughter rock is about 14% greater than the volume of its parent.

Replacement of plagioclase could have been accomplished by a combination of the following two equations.

$$NaAlSi_3O_8 + K^+ = KAlSi_3O_8 + Na^+$$

$$CaAl_2Si_2O_8 + 2K^+ + 4SiO_2 = 2KAlSi_3O_8 + Ca^{2+}$$

Conversion of the albite component of plagioclase to adularia involves a simple alkali exchange, but conversion of the anorthite component requires additional silica if Al is immobile. During metasomatism of the dacite of Cady Mountains, some of the silica was derived from the rock itself and some was introduced from the outside, as shown by the calculation diagramed in Figure 9. If components other than quartz and feldspars are ignored, then on a CIPW normative basis, rock 13-21C has 0.216 moles quartz, 0.088 moles orthoclase, 0.17 moles albite, and 0.0647 moles anorthite per 100 g rock. Conversion of albite to orthoclase can proceed by simple ion exchange, but conversion of anorthite to orthoclase requires 0.259 moles (= 4 × 0.0647) of silica if Al is immobile. The presence of abundant jasper veins indicates that silica was mobile during the alteration process. The rock

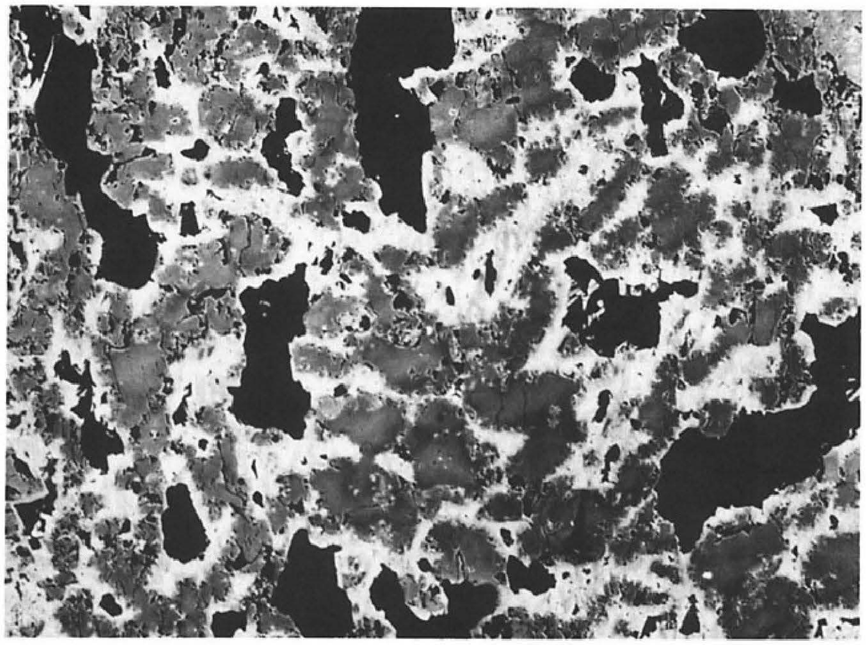

**Figure 6. Backscatter scanning electron photomicrograph of the grainy portion of a plagioclase phenocryst undergoing replacement by adularia. White areas are adularia; gray areas are plagioclase; black areas are holes. Subtle variations in gray tone may be a result of specimen topography. In metasomatized plagioclases, the ratio of adularia to plagioclase generally increases outward. Width of field, 0.1 mm.**

contains 0.216 moles of free silica, and so 0.043 moles must be introduced from outside. The volume increase produced by this reaction is approximately 10 vol%.

The volume increase implied by the calculation above and by the composition-volume calculations can account for the highly shattered nature of the metasomatized rocks (Fig. 4). If solutions gain access to the rock via cooling joints and other cracks, as shown in Figure 4B, then the volume increase can induce stresses at crack tips and propagate the cracks through the rock. This process can effectively shatter large bodies and promote further ingress of solutions.

### Isotopic Changes

The whole-rock isotopic composition of oxygen was affected by metasomatism (Fig. 10). In general, $\delta^{18}O$ correlates positively with $K_2O$, although the sample with the highest measured $K_2O$ has relatively low $\delta^{18}O$ (Table 4). This sample is also enriched in iron over most samples of the dacite of Cady Mountains (Table 4), and so its low $\delta^{18}O$ may result from the tendency of iron-bearing compounds to concentrate light oxygen (Chapin and Lindley, 1986). Chapin and Lindley (1986) and Kerrich and Rehrig (1987) reported similar correlations between K enrichment and whole-rock $\delta^{18}O$ in metasomatized rocks. $^{18}O$ is also elevated in quartz ($\delta^{18}O$ = 15.18) and in jasper ($\delta^{18}O$ = 13.58) from jasper-filled breccia zones.

Measured $^{87}Sr/^{86}Sr$ values from the dacite of Cady Mountains indicate that the isotopic composition of Sr was variably affected by metasomatism. Sample A3-3B, the sample with the highest measured $K_2O$, has highly elevated $^{87}Sr/^{86}Sr$ (0.71309; Table 4). Corrected for 20 m.y. of *in situ* growth, this value decreases to 0.7110, which is significantly greater than the value of 0.7089 for fresh dacite. This implies that the metasomatic fluid carried Sr having a high $^{87}Sr/^{86}Sr$ ratio. In contrast, highly metasomatized sample 13-21B, when corrected for 20 m.y. of growth, has a ratio of only 0.7084, which is slightly less than the ratio in fresh dacite.

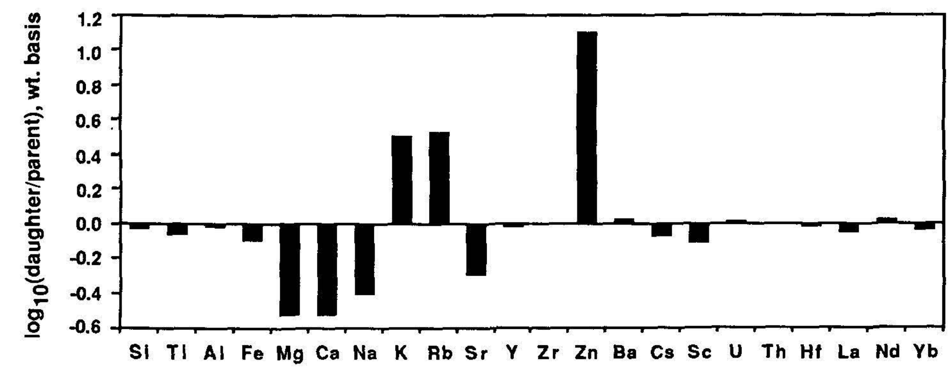


**Figure 7. Bar chart of elemental changes during metasomatism for dacite pair 13-21C/13-21B of Table 4. The ordinate gives $\log_{10}$ of the weight ratio (concentration in metasomatized rock)/(concentration in protolith).**

TABLE 3. UNIT-CELL PARAMETERS FOR METASOMATIC ADULARIA

| Sample | 13-21B | 13-21F | 13-21E | Mean |
|---|---|---|---|---|
| a (Å) | 8.600 | 8.587 | 8.593 | 8.593 |
| b (Å) | 13.004 | 12.999 | 13.006 | 13.003 |
| c (Å) | 7.186 | 7.180 | 7.184 | 7.183 |
| $\beta$ | 116.10° | 115.84° | 116.00° | 115.98° |
| volume, $Å^3$ | 721.7 | 721.3 | 721.6 | 721.5 |
| n | 19 | 15 | 20 | |
| wt% $K_2O$ | 11.71 | 7.79 | 6.14 | |

*Note:* n = number of peaks used in unit-cell refinement. Samples taken from locality shown in Figure 4A. Wt% $K_2O$ refers to whole-rock value.

## ORIGIN OF THE METASOMATIC ROCKS

### Pressure-Temperature Conditions

Metasomatism probably occurred at shallow depths (<1 or 2 km), on the basis of the known thickness of rocks above the metasomatized zones. Because metasomatism is accompanied by a large volume increase, significant confining

TABLE 4. COMPOSITIONAL COMPARISON OF REPRESENTATIVE SETS OF FRESH AND METASOMITIZED ROCKS FROM THE SLEEPING BEAUTY AREA

| Rock type | Dacite (DCM) | | Dacite (DCM) | | | | Basalt (FAS) | | Rhyodacite (FAS) | |
|---|---|---|---|---|---|---|---|---|---|---|
| Sample | AG-2 | A3-3B | 13-21C | 13-21E | 13-21F | 13-21B | 12-3 | 14-19* | 13-34* | 13-23 |
| $SiO_2$ | 63.2 | 58.0 | 63.8 | 62.8 | 61.7 | 60.2 | 49.7 | 58.1 | 65.1 | 70.6 |
| $TiO_2$ | .76 | .55 | .88 | .83 | .80 | .77 | 2.63 | .99 | .42 | .38 |
| $Al_2O_3$ | 16.4 | 16.6 | 17.6 | 17.2 | 17.0 | 17.2 | 16.1 | 15.2 | 16.3 | 13.3 |
| $Fe_2O_3{}^t$ | 5.91 | 7.56 | 5.04 | 5.01 | 4.75 | 4.05 | 12.53 | 5.21 | 2.76 | 4.52 |
| MgO | 1.49 | .44 | .82 | .32 | .32 | .25 | 4.51 | .33 | 1.04 | .37 |
| CaO | 3.69 | .35 | 3.71 | 2.71 | 2.24 | 1.12 | 8.23 | 3.81 | 3.23 | .73 |
| $Na_2O$ | 5.01 | .98 | 4.67 | 4.17 | 3.24 | 1.86 | 3.67 | 1.19 | 4.38 | 1.33 |
| $K_2O$ | 3.20 | 13.36 | 3.69 | 6.14 | 7.79 | 11.71 | 1.53 | 11.31 | 3.44 | 8.95 |
| LOI | 0.3 | . . | . . | . . | . . | . . | −1.1 | . . | 2.7 | . . |
| Total | 100.0 | 97.8 | 100.2 | 99.2 | 97.8 | 97.2 | 97.8 | 96.1 | 99.7 | 100.2 |
| Rb | 115 | 605 | 130 | 228 | 289 | 433 | 31 | 373 | 168 | 361 |
| Sr | 450 | 245 | 492 | 419 | 375 | 256 | 557 | 209 | 1250 | 103 |
| Y | 35 | 33 | 33 | 33 | 31 | 32 | 30 | 26 | 20 | 12 |
| Zr | 339 | 334 | 337 | 338 | 337 | 338 | 202 | 251 | 158 | 139 |
| Zn | 59 | 731 | 74 | 880 | 805 | 930 | 114 | 122 | 57 | 53 |
| Ba | 981 | 1779 | 1190 | 1226 | 1437 | 1239 | 500 | 1154 | 605 | 947 |
| La | 43.9 | 13.04 | 42.5 | . . | 41.4 | 38.4 | 25.7 | 49.3 | . . | 20.3 |
| Ce | 81.3 | 32.0 | 81.3 | . . | 71.1 | 74.1 | 52.7 | 88.2 | . . | 36.0 |
| Nd | 37.1 | 14.4 | 35.3 | . . | 37.2 | 36.9 | 26.7 | 40.8 | . . | 16.9 |
| Sm | 6.82 | 3.12 | 7.13 | . . | 6.95 | 6.70 | 6.48 | 6.91 | . . | 2.97 |
| Eu | 1.91 | 1.2 | 2.07 | . . | 2.05 | 1.54 | 2.29 | 1.85 | . . | 0.75 |
| Tb | 0.85 | 0.5 | 0.871 | . . | 0.829 | 0.775 | 1.07 | 0.679 | . . | 1.0 |
| Yb | 2.40 | 1.54 | 2.13 | . . | 2.05 | 1.96 | 2.65 | 1.70 | . . | 0.65 |
| Lu | 0.367 | 0.26 | 0.350 | . . | 0.297 | 0.277 | 0.373 | 0.270 | . . | 0.13 |
| Cs | 19.6 | 14.3 | 4.93 | . . | 3.88 | 4.22 | 1.45 | 3.47 | . . | 6.97 |
| Sc | 6.63 | 5.12 | 7.24 | . . | 6.25 | 5.65 | 21.4 | 9.41 | . . | 3.9 |
| U | 2.22 | 2.57 | 2.45 | . . | 1.92 | 2.52 | 0.9 | 2.44 | . . | 2.81 |
| Th | 9.26 | 10.0 | 9.15 | . . | 9.31 | 9.18 | 3.30 | 9.60 | . . | 8.82 |
| Hf | 7.94 | 8.47 | 8.37 | . . | 8.43 | 8.20 | 5.56 | 6.22 | . . | 3.4 |
| $^{87}Sr/^{86}Sr$ | .70885 | .71309 | .70893 | . . | . . | .70983 | .70550 | . . | . . | . . |
| $\rho$ (g/cm$^3$) | 2.622 | . . | 2.530 | . . | 2.464 | 2.420 | 2.794 | 2.565 | . . | 2.581 |
| $\delta^{18}O$ | 8.23 | 8.82 | 9.87 | 10.93 | 10.33 | 13.16 | . . | . . | . . | . . |

*Note*: . . = not determined. Major-element and Rb, Sr, Y, Zr, Zn, Ba analyses by X-ray fluorescence and, on some samples, by atomic absorption for Na and Mg; rare earths, Cs, Sc, U, Th, and Hf by instrumental neutron-activation analysis. DCM = dacite of Cady Mountains; FAS = formation of Argos Station. Oxides in weight percent; trace elements in parts per million. Isotopic ratios are measured values (not corrected for age). $\delta^{18}O$ measured relative to standard mean ocean water.

Dacite group 13-21C, E, F, B was taken from the locality shown in Figure 4A; B is a clast in the breccia zone, E and F are from the margin of the breccia zone, and C was taken from relatively fresh dacite 2 m from the breccia zone. Other pairs were not taken from the same flows, and thus, in each case, the protolith of the metasomatized rock can be considered to be only a rough equivalent of the fresh rock.

*Contains modal calcite.

pressure would inhibit the metasomatic reactions. This pressure effect cannot be quantified until more is known about the thermodynamic properties of the fluid phase.

Several aspects of the metasomatism indicate that it probably occurred at temperatures of a few hundred degrees Celsius or less. These are:

(1) The general increase in whole-rock $\delta^{18}O$ values with $K_2O$. If the metasomatized rocks are considered to be nearly pure adularia with $\delta^{18}O$ = 13, then an estimate of the temperature of alteration, based on the fractionation of oxygen isotopes between alkali feldspar and water (O'Neil and Taylor, 1967), can be obtained as a function of the assumed $\delta^{18}O$ of the hydrothermal fluid. Because meteoric waters and most hydrothermal waters have $\delta^{18}O < 0$, these calculations indicate that metasomatism probably occurred at temperatures less than approximately 150 °C.

(2) The nearly pure composition of the adularia. At low temperatures, the solvus between Na-rich and K-rich feldspars expands such that K-rich and Na-rich feldspars show virtually no solid solution. The solvus calculated by Waldbaum and Thompson (1969) predicts that at 200 °C, K-rich feldspar will tolerate only a few mole percent Na-rich feldspar in solution.

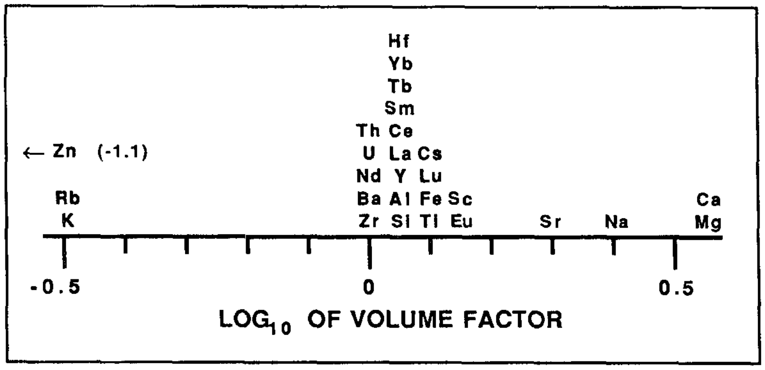


**Figure 8. Summary of volume factors (= volume metasomatized rock/volume protolith) needed for immobility of an element during metasomatic conversion of sample 13-21C to sample 13-21B. Clustering of volume factors indicates that most elements could have been immobile if metasomatism was accompanied by a volume increase of about 14 vol%.**

(3) The presence of adularia as the predominant alteration phase. Thermochemical data indicate that K-feldspar should be stable at low temperatures even in the presence of aqueous solutions with high $Na^+/K^+$ ratios (Orville, 1963; Munhá and others, 1980). The relevant reaction is $K^+_{aq} + NaAlSi_3O_8 = Na^+_{aq} + KAlSi_3O_8$. Data from Robie and others (1978) for this reaction give (25 °C) $\Delta G^0 = -12{,}700$ J/mol, $\Delta S^0 = -36.1$ J/mol·K (standard states are disordered feldspars and 1-molal aqueous solutions). Calculated values for the equilibrium constant are 167 at 25 °C and 5 at 200 °C. The feldspar end members are essentially pure at low temperature (unit activity), and so the equilibrium constant is equal to the ratio of the activities of the aqueous species ($K = a_{Na^+}/a_{K^+}$). Because the activity coefficients of $K^+$ and $Na^+$ are similar in aqueous solutions (Garrels and Christ, 1965, p. 368–369), the equilibrium constant can be approximated by the atomic Na/K ratio in the fluid. These data indicate that K-feldspar will be favored at low temperatures even in the presence of an aqueous fluid with a high $Na^+/K^+$ ratio. At higher temperatures, Na-feldspar is favored owing to the rapid decrease in the equilibrium constant with increasing temperature.

### Timing

At least some metasomatism occurred before eruption of the dacite of Cady Mountains (see below). The Peach Springs Tuff is not noticeably metasomatized, and so all metasomatism probably predated its deposition. This conclusion is tentative because of the patchy occurrence of metasomatized zones and the relatively local distribution of the tuff.

Field evidence indicates that metasomatism occurred in at least two pulses. A bright red arkose layer within the formation of Argos Station at the eastern base of hill 2547, sec. 28, T. 8 N., R. 7 E., is composed almost entirely of adularia grains and contains about 10.5 wt% $K_2O$. Because ash-flow tuff immediately above and below the arkose is unmetasomatized, it is unlikely that the high-K arkose was produced by *in situ* metasomatism of a sandstone or arkose; it was most likely derived by erosion of a preexisting metasomatized volcanic rock. Cathodoluminescence study of the arkose (G. Hileman, 1986, written commun.) supports this interpretation. Thus, because the arkose underlies metasomatized rocks of the dacite of Cady Mountains, at least two distinct (but possibly closely spaced) periods of metasomatism are required.

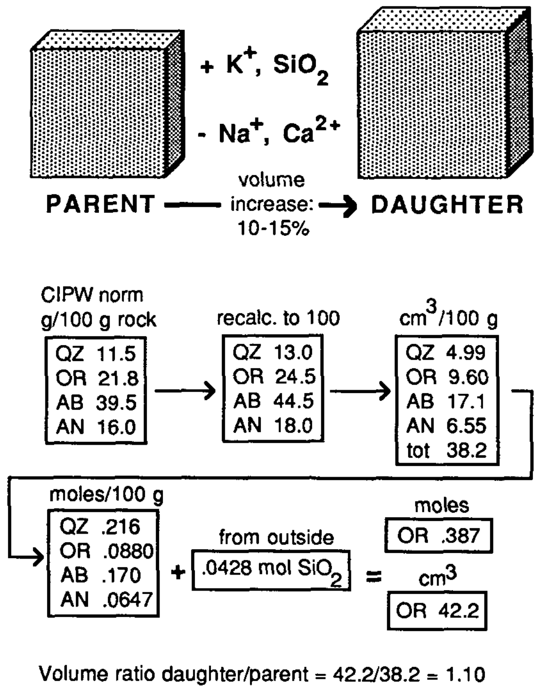


**Figure 9. Proposed element mobility and volume change during metasomatism of the dacite of Cady Mountains. If Al is immobile, then conversion of anorthite to orthoclase requires introduction of $SiO_2$. Free $SiO_2$ in the dacite is insufficient to complete the reaction, and so some must have been introduced from outside. The calculated volume increase implied by this model (≈10%) is similar to that calculated using composition/volume relations (Fig. 8).**

### Model

On the basis of their work in the Rio Grande rift, Chapin and Lindley (1986) proposed that alkaline, saline brines are responsible for potassic metasomatism in extensional basins. In their model, metasomatism occurs diagenetically under closed basins as brines percolate downward into extended, fractured rocks. This model is successful in explaining many of the features of metasomatized areas, including the Sleeping Beauty area. In addition, the brine model can explain the possible presence of excess B in the metasomatic feldspars (Sheppard and Gude, 1973). Two aspects of metasomatism in the Sleeping Beauty area do not conform to Chapin and Lindley's model, however.

The first problem is that lacustrine rocks of the proper age are not present. The only lacustrine sediments in the area (Hector Formation) were deposited after the Peach Springs Tuff blanketed the area and thus after at least some, and probably all, metasomatism occurred. Older sedimentary rocks in the area are uncommon and are predominantly alluvial. As a rule, lacustrine deposition within the Mojave volcanic belt generally commenced after most volcanism had ceased. The second problem is that the brine model does not account for the jasper-filled breccia zones and their clear association with metasomatism. Because the breccia zones are not found outside metasomatized zones, they cannot be passive conduits through which brines percolated.

An alternative model was proposed by Chapin and Glazner (1983) and Bartley and Glazner (1985). In this model, the K is derived from basement rocks beneath the volcanic pile, and the metasomatized zones are remnants of the upper parts of hydrothermal systems associated with volcanism and faulting. Circulating meteoric waters pick up $K^+$ from basement rocks in exchange for $H^+$, producing the characteristic low-grade metamorphic assemblages (sericite, chlorite, clinozoisite, clays) seen beneath detachment faults (Davis, 1980; Davis and others, 1980). $K_2O$ depletion is observed in footwall rocks from some detachment-fault complexes; for example, mylonitic granodiorite in the footwall of the Waterman Hills detachment fault near Barstow has lost approximately 2 wt% $K_2O$ relative to unaltered granodiorite (A. F. Glazner and J. M. Bartley, unpub. data), and B. John (1983, oral commun.) has measured as much as 3 wt% $K_2O$ loss in footwall rocks of the Chemehuevi Mountains extensional fault complex, 150 km to the east. As the waters ascend, they deposit the $K^+$ in cooler upper-plate volcanic rocks, receiving $Na^+$ and $Ca^{2+}$ in exchange. The $Na^+$ and $Ca^{2+}$ (and perhaps $Sr^{2+}$ as well) are then carried to the surface in hot springs. Metasomatism thus reflects thermal control of the distribution of $K^+$ and $Na^+$ between alkali feldspar and coexisting fluid (Orville, 1963).

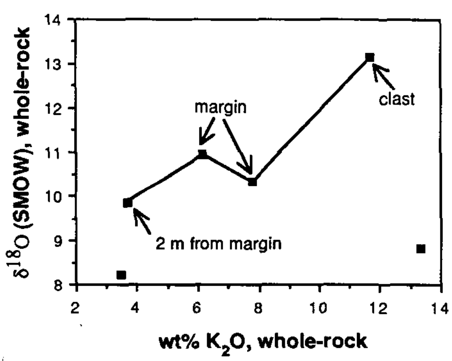


**Figure 10. Plot of $\delta^{18}O$ versus wt% $K_2O$ for 6 samples of the dacite of Cady Mountains. Points connected by a line are from the locality shown in Figure 4A. Sample labeled "2 m from margin" is from 2 m from the breccia zone shown in Figure 4A (sample 13-21C of Table 4); samples labeled "margin" are from the margins of the breccia zone; sample labeled "clast" is a clast from within the breccia zone (sample 13-21B of Table 4).**

Bartley and Glazner (1985) proposed that the jasper-filled breccia zones represent natural hydrofracturing of the rocks in a periodically sealed geothermal system. In this model, which is based on the observation that tilted Tertiary rocks above low-angle normal faults are commonly K metasomatized, the pore pressure that is developed facilitates formation of low-angle normal faults. Failure of the seal in the geothermal system causes tensile fracturing and floods shallow levels of the system with a K-, Si-, Fe-rich fluid, producing the jasper-filled breccia zones and attendant potassic metasomatism.

## CONCLUSIONS

(1) The record of volcanism in the Sleeping Beauty area commences with eruption of andesite and dacite from a large stratovolcano complex. Volcanism then shifted to eruption of alkali basalt and basaltic andesite from several cinder cones which were arranged around the periphery of the stratovolcano. These basalts are interbedded with silicic tuffs which were derived from the east, outside the area. Local volcanism ended with eruption of the dacite of Cady Mountains. Feeder dikes for this dacite were not found; its source is unknown. The area was then blanketed by the Peach Springs Tuff. Lacustrine, fluvial, and alluvial sedimentation, represented by the Hector Formation, followed deposition of the tuff.

(2) Volcanism in the area occurred during a short time span, approximately between 20 and 18.5 m.y. ago. This interval apparently coincided with the transition from subduction to transform-fault tectonics off the coast of California.

(3) Tertiary rocks in the area are tilted to the southwest and are cut by numerous northwest- to north-trending faults. The structural style is similar to that seen in the upper plates of low-angle normal fault complexes, although deformation was not strictly by a "tilted-book" mechanism. No major low-angle normal faults were found, but such faults occur in ranges to the west and project under the Sleeping Beauty area. Tilting occurred before deposition of the Peach Springs Tuff and thus was roughly contemporaneous with volcanism. The timing of folding about gently southeast-plunging axes is not well constrained.

(4) Intense potassic metasomatism affected all units older than the Peach Springs Tuff and occurred in at least two distinct pulses. Metasomatism apparently occurred at about the same time that the rocks were tilted, and zones of metasomatism are parallel to major faults. Metasomatism is expressed chemically by enrichment in K, Rb, and Zn and by depletion in Ca, Na, and Mg. Mineralogical changes include replacement of plagioclase by end-member K-feldspar and pervasive oxidation. Metasomatism occurred at shallow depth (<1 or 2 km) and low temperature (<150 °C) and was accompanied by a volume increase of approximately 10%–15%, which promoted brecciation.

(5) The K added during metasomatism may have been derived from hydrogen-metasomatized rocks deeper in the complex or from percolating closed-basin brines.

## ACKNOWLEDGMENTS

The work was supported by grants from the National Science Foundation (EAR-8219032 to the author and EAR-7816413 to A. L. Boettcher); the Petroleum Research Fund, which is administered by the American Chemical Society; the Geological Society of America; and the Society of Sigma Xi. The Department of Earth and Space Sciences at the University of California, Los Angeles, and the Department of Geology at Pomona College also provided substantial support. Encouragement and logistical support from D. M. Miller and K. A. Howard of the U.S. Geological Survey were indispensable. J. R. O'Neil offered the use of his laboratory and expertise for the oxygen analyses. J. M. Bartley, J. R. Butler, J. E. Nielson, and R. D. Turner reviewed an early version of the manuscript, and K. L. Kimball, G. A. Mahood, and C. Simpson provided constructive reviews of the submitted version. A. K. Baird, J. M. Bartley, A. L. Boettcher, B. J. Bilodeau, C. E. Chapin, S. N. Ehrenberg, C. E. Jacobson, R. L. Jones, D. M. Miller, M. S. Olney, S. S. Sorensen, and A. L. Stork were all of great assistance in the field and in the laboratory.

### *REFERENCES CITED*

Appleyard, E. C., and Woolley, A. R., 1979, Fenitization: An example of the problems of characterizing mass transfer and volume changes: Chemical Geology, v. 26, p. 1–15.

Armstrong, R. L., and Higgins, R. E., 1973, K-Ar dating of the beginning of Tertiary volcanism in the Mojave Desert, California: Geological Society of America Bulletin, v. 84, p. 1095–1100.

Bailey, D. K., 1960, Carbonatites of the Rufunsa Valley, Feira district: Northern Rhodesia Geological Survey Bulletin, v. 5, 86 p.

Bartley, J. M., and Glazner, A. F., 1985, Hydrothermal systems and Tertiary low-angle normal faulting in the southwestern United States: Geology, v. 13, p. 562–564.

——— 1987, Tertiary deformation beneath the Waterman detachment, central Mojave Desert, California: Geological Society of America Abstracts with Programs, v. 19, p. 582.

Brooks, W. E., 1986, Distribution of anomalously high $K_2O$ volcanic rocks in Arizona: Metasomatism at the Picacho Peak detachment fault: Geology, v. 14, p. 339–342.

Brown, P. E., 1964, The Songwe scarp carbonatite and associated feldspathization in the Mbeya Range, Tanganyika: Geological Society of London Quaterly Journal, v. 120, p. 223–240.

Burchfiel, B. C., Walker, D., Davis, G. A., and Wernicke, B., 1983, Kingston Range and related detachment faults—A major "breakaway" zone in the southern Great Basin: Geological Society of America Abstracts with Programs, v. 15, p. 536.

Chapin, C. E., and Glazner, A. F., 1983, Widespread $K_2O$ metasomatism of Cenozoic volcanic and sedimentary rocks in the southwestern United States: Geological Society of America Abstracts with Programs, v. 15, p. 282.

Chapin, C. E., and Lindley, J. I., 1986, Potassium metasomatism of igneous and sedimentary rocks in detachment terranes and other sedimentary basins: Economic implications: Arizona Geological Society Digest, v. 16, p. 118–126.

Davis, G. A., Anderson, J. L., Frost, E. G., and Shackelford, T. J., 1980, Mylonitization and detachment faulting in the Whipple-Buckskin-Rawhide Mountains terrane, southeastern California and western Arizona: Geological Society of America Memoir 153, p. 79–129.

Davis, G. H., 1980, Structural characteristics of metamorphic core complexes, southern Arizona: Geological Society of America Memoir, v. 153, p. 35–77.

Dibblee, T. W., Jr., 1967, Geologic map of the Broadwell Lake quadrangle, San Bernardino County, California: U.S. Geological Survey Map I-478.

Dokka, R. K., 1986, Patterns and modes of early Miocene crustal extension, central Mojave Desert, California: Geological Society of America Special Paper 208, p. 75–95.

Durrell, C., 1953, Celestite deposits near Ludlow, San Bernardino County, California: California Division of Mines and Geology Bulletin, v. 32, p. 37–48.

Garfunkel, Z., 1974, Model for the late Cenozoic tectonic history of the Mojave Desert, California, and for its relation to adjacent regions: Geological Society of America Bulletin, v. 85, p. 1931–1944.

Garrels, R. M., and Christ, C. L., 1965, Solutions, minerals, and equilibria: San Francisco, Freeman, Cooper and Company, 450 p.

Garson, M. S., 1962, The Tundulu carbonatite ring-complex in southern Nyasaland: Nyasaland Geological Survey Department Memoir, v. 2, 248 p.

Glazner, A. F., 1979, Geochemistry of ultrapotassic metasomatism in the Sleeping Beauty volcanic area, central Mojave Desert, California: Geological Society of America Abstracts with Programs, v. 11, p. 79–80.

——— 1988, Recycling of continental crust in Miocene volcanic rocks from the Mojave block, southern California: Geological Society of America Special Paper, "The nature and origin of Cordilleran magmatism" (in press).

Glazner, A. F., and Bartley, J. M., 1984, Timing and tectonic setting of Tertiary low-angle normal faulting and associated magmatism in the southwestern United States: Tectonics, v. 3, p. 385–396.

Glazner, A. F., and Stork, A. L., 1976, Ultrapotassic, silica-rich, Tertiary volcanic rocks from the Mojave Desert, California: Geological Society of America Abstracts with Programs, v. 8, p. 886.

Glazner, A. F., Nielson, J. E., Howard, K. A., and Miller, D. M., 1986, Correlation of the Peach Springs Tuff, a large-volume Miocene ignimbrite sheet in California and Arizona: Geology, v. 14, p. 840–843.

Glazner, A. F., Dent, S. B., and Bartley, J. M., 1987, Miocene detachment fault in the Waterman Hills, central Mojave Desert, California: Geological Society of America Abstracts with Programs, v. 19, p. 381–382.

Gresens, R. L., 1967, Composition-volume relationships of metasomatism: Chemical Geology, v. 2, p. 47–65.

Kastner, M., and Siever, R., 1979, Low temperature feldspars in sedimentary rocks: American Journal of Science, v. 279, p. 435–479.

Kerrich, R., and Rehrig, W., 1987, Fluid motion associated with Tertiary mylonitization and detachment faulting: $^{18}O/^{16}O$ evidence from the Picacho metamorphic core complex, Arizona: Geology, v. 15, p. 58–62.

Koski, R. A., Chesterman, C. W., Silberman, M. I., and Fabbi, B. P., 1978, Hydrothermal adularia at Bodie, Mono County, California: U.S. Geological Survey Open-File Report, v. 78-942.

Kroll, H., and Ribbe, P. H., 1983, Lattice parameters, composition and Al, Si order in alkali feldspars, *in* Ribbe, P. H., ed., Feldspar mineralogy: Reviews in mineralogy, volume 2 (2nd edition): Washington, D.C., Mineralogical Society of America, p. 57–99.

Martin, R. F., 1971, Disordered authigenic feldspars of the series $KAlSi_3O_8$-$KBSi_3O_8$ from southern California: American Mineralogist, v. 56, p. 281–291.

Moody, J. D., and Hill, M. J., 1956, Wrench-fault tectonics: Geological Society of America Bulletin, v. 67, p. 1207–1246.

Munhá, J., Fyfe, W. S., and Kerrich, R., 1980, Adularia, the characteristic mineral of felsic spilites: Contributions to Mineralogy and Petrology, v. 75, p. 15–19.

O'Neil, J. R., and Taylor, H. P., Jr., 1967, The oxygen isotope and cation exchange chemistry of feldspars: American Mineralogist, v. 52, p. 1414–1437.

Orville, P. M., 1963, Alkali ion exchange between vapor and feldspar phases: American Journal of Science, v. 261, p. 201–237.

Rehrig, W. A., Shafiqullah, M., and Damon, P. E., 1980, Geochronology, geology, and listric normal faulting of the Vulture Mountains, Maricopa County, Arizona: Arizona Geological Society Digest, v. 12, p. 89–110.

Robie, R. A., Hemingway, B. S., and Fisher, J. R., 1978, Thermodynamic properties of minerals and related substances at 298.15 K and 1 bar ($10^5$ pascals) pressure and at higher temperatures: U.S. Geological Survey Bulletin, v. 1452, 456 p.

Shafiqullah, M., Lynch, D. J., and Damon, P. E., 1976, Geology, geochronology and geochemistry of the Picacho Peak area, Pinal County, Arizona: Arizona Geological Society Digest, v. 10, p. 305–324.

Sheppard, R. A., and Gude, A. J., III, 1965, Potash feldspar of possible economic value in the Barstow Formation, San Bernardino County, California: U.S. Geological Survey Circular, v. 500, p. 1–7.

——— 1973, Boron-bearing potassium feldspar of authigenic origin in closed-basin deposits: U.S. Geological Survey Journal of Research, v. 1, p. 377–382.

Trask, P. D., 1950, Geologic description of the manganese deposits of California: California Division of Mines and Geology Bulletin, v. 152.

Waldbaum, D. R., and Thompson, J. B., Jr., 1969, Mixing properties of sanidine crystalline solutions: IV. Phase diagrams from equations of state: American Mineralogist, v. 54, p. 1274–1298.

Wells, R. E., and Hillhouse, J. W., 1986, Paleomagnetism of the Peach Springs Tuff and correlative outcrops from Barstow, California to the Colorado Plateau, Arizona: Geological Society of America Abstracts with Programs, v. 18, p. 421.

Wernicke, B., and Burchfiel, B. C., 1982, Modes of extensional tectonics: Journal of Structural Geology, v. 4, p. 105–115.

Woodburne, M. O., Tedford, R. H., Stevens, M. S., and Taylor, B. E., 1974, Early Miocene mammalian faunas, Mojave Desert, California: Journal of Paleontology, v. 48, p. 6–26.

Young, R. A., and Brennan, W. J., 1974, Peach Springs Tuff: Its bearing on structural evolution of the Colorado Plateau and development of Cenozoic drainage in Mohave County, Arizona: Geological Society of America Bulletin, v. 85, p. 83–90.

MANUSCRIPT RECEIVED BY THE SOCIETY MARCH 3, 1987
REVISED MANUSCRIPT RECEIVED AUGUST 25, 1987
MANUSCRIPT ACCEPTED AUGUST 28, 1987